OPEN ACCESS Journal of Animal Health and Production

Research Article

Effect of Nano Encapsulated Chitosan- Collagen Hydrogel on Healing of Injured Achilles Tendon in a Rabbit Model

Zainab A. Fadhil*, Areeg K. Mahdi

Departments of Surgery and Obstetrics, College of Veterinary Medicine, University of Baghdad, Iraq.

Abstract | Tendon injuries pose a significant clinical challenge due to their limited intrinsic healing capacity, often resulting in fibrotic scar formation and impaired mechanical function. This study investigates the efficacy of nano encapsulated chitosan-collagen hydrogel (NECCH) compared to untreated tendon in enhancing the healing process of injured Achilles tendons in a rabbit model. A total of 40 adult male rabbits were used and divided into two groups: (A) control (untreated), (B) NECCH-treated. The experimental model involved standardized Achilles tenotomy followed by tenorrhaphy using the modified Kessler technique. The nano encapsulated chitosan-collagen (0.3 ml of chitosan (2 w/v%) and collagen-I (4 mg/ml) hydrogel were locally applied at the repair site to assess their regenerative potential. Post-operative evaluations included clinical examinations, ultrasonography, macroscopic and histopathological assessments, over 12 weeks. The results demonstrated that the treatment group exhibited superior tendon healing compared to the control group, as evidenced by reduced inflammatory response, enhanced tendon gliding, and more organized collagen deposition following NECCH treatment. Ultrasound imaging confirmed enhanced tendon integrity and reduced adhesion formation in the treated groups. These findings suggest that NECCH offers a promising therapeutic strategy for tendon repair, providing a biocompatible scaffold that facilitates tissue regeneration and functional restoration.

Keywords | Achilles tendon injury, Nano-encapsulated Chitosan-collagen hydrogel, Rabbit model, Tendon regeneration

Received | December 20, 2025; **Accepted** | January 02, 2026; **Published** | March 04, 2026
***Correspondence** | Zainab A. Fadhil, Departments of Surgery and Obstetrics, College of Veterinary Medicine, University of Baghdad, Iraq; **Email:** Zainab.Abbas2202m@covm.uobaghdad.edu.iq
Citation | Fadhil ZA, Mahdi AK (2026). Effect of nano encapsulated chitosan- collagen hydrogel on healing of injured achilles tendon in a rabbit model. J. Anim. Health Prod. 14(2): 416-427.
DOI | https://dx.doi.org/10.17582/journal.jahp/2026/14.2.416.427
ISSN (Online) | 2308-2801

INTRODUCTION

Tendon injuries are a frequent clinical challenge, especially in orthopedic and sports medicine (Al-Falahi, 2016). The Achilles tendon, due to its limited vascular supply and low cellularity, is particularly prone to poor healing outcomes, often resulting in fibrotic scar formation and loss of mechanical function (Andarawis-Puri *et al*., 2015; Galatz *et al*., 2015). Conventional approaches such as surgical repair and physical therapy have shown limited success in restoring tendon integrity (Millar *et al*., 2017). Al-Falahi (2016) reported that platelet rich fibrin matrix significantly improved tendon organization and reduced inflammation in tendon injuries. Their findings support the concept that biologically derived treatments can accelerate the healing process.

Recent advancements in tissue engineering have introduced nanotechnology-based biomaterials that offer unique physicochemical properties capable of enhancing tendon regeneration (Parchi *et al*.,2016; Alhtheal and Azhar, 2018). Among these, chitosan and collagen-based hydrogels have gained significant attention for their biocompatibility, biodegradability, and support for extracellular matrix (ECM) remodeling (Sánchez-Cid *et al*., 2022).

Chitosan, a natural polysaccharide, possesses antibacterial, anti-inflammatory, and regenerative properties. It has been used in various biomedical applications including wound dressings, hydrogels, drug delivery systems, and scaffolds for tissue engineering (Ricard-Blum, 2011; Salih *et al*., 2015: Zhang *et al*., 2023). *In vivo*, chitosan supports cell attachment and collagen deposition, and its hydrogels have been shown to prevent scar formation and aid in nerve and tendon healing (Xia *et al*., 2022).

Collagen, the predominant structural protein in tendons, plays a crucial role in cell adhesion, tissue repair, and regeneration. It is widely used in wound healing products, orthopedic scaffolds, and controlled drug delivery systems due to its ability to support fibroblast proliferation and ECM synthesis (Lee *et al*., 2001; Ricard-Blum, 2011; Hu *et al*., 2023).

Combining chitosan and collagen into nano-encapsulated hydrogel formulations provides a novel controlled-release system capable of modulating inflammation, enhancing fibroblast activity, and accelerating tissue remodeling. Promising outcomes have been reported in models using chitosan/collagen hydrogels with tendon stem cells or aligned nanofiber scaffolds, improving structural integration and healing after Achilles tendon injuries (Deepthi *et al*., 2016; Yang *et al*., 2017; Parchi *et al*., 2016). Furthermore, nanoparticle-based platforms are known to improve the bioavailability and localized action of therapeutic agents (Egwe *et al*., 2024).

This study aimed to evaluate the healing efficacy of nano-encapsulated chitosan-collagen hydrogel (NECCH) in a rabbit model of Achilles tendon tenorrhaphy. Clinical, ultrasonographic, macroscopic, and histopathological assessments were employed to assess the regenerative impact of the hydrogel on tendon repair.

MATERIALS AND METHODS

Experimental animals

All procedures for this study were approved by the Ethics Committee of Baghdad University College of Veterinary Medicine in accordance with ethical standards for animal welfare (541). Forty adult male local rabbits, weighing 1.5-2 kg, were housed in individual standard cages, in which each cage size measured 60 × 50 × 45 (length × width × height), with free access to food that is considered as a standard laboratory and nutritionally balanced pellet diet with fresh water at the animal house of the College of Veterinary Medicine. Rabbits were dewormed with Ivermectin at a dose of 0.2mg/kg subcutaneously, followed by a second dose on 14th day, with a second dose given 14 days later.

Surgical technique

All operations were conducted under strict aseptic conditions. All rabbits underwent Achilles tendon transection and repair under general anesthesia to minimize pain and distress. Anesthesia was induced via intramuscular injection of xylazine at 5 mg/kg and ketamine at 35 mg/kg (Hassan *et al*., 2024). The right hind limb was shaved, aseptically prepared and positioned in lateral recumbency for optimal surgical exposure.

A longitudinal paratendinous skin incision was made to expose the Achilles tendon (Figure 1A). A full-thickness tenotomy was performed at the tendon's midpoint using a scalpel blade. Tendon repair was achieved using the modified Kessler suture technique with USP 4-0 polypropylene (Figure 1B), ensuring proper tendon coaptation with minimal tension at the repair site (Millar *et al*., 2021). In the control group (Group A), the tenorrhaphy site was left untreated. In the NECCH-treated group (Group B), the prepared NECCH was applied locally to fully cover the suture line, ensuring even distribution across the repair site (Figure 1C). Skin closure was performed using a subcuticular suture pattern with 3-0 polydioxanone to promote optimal wound healing and minimize postoperative irritation.

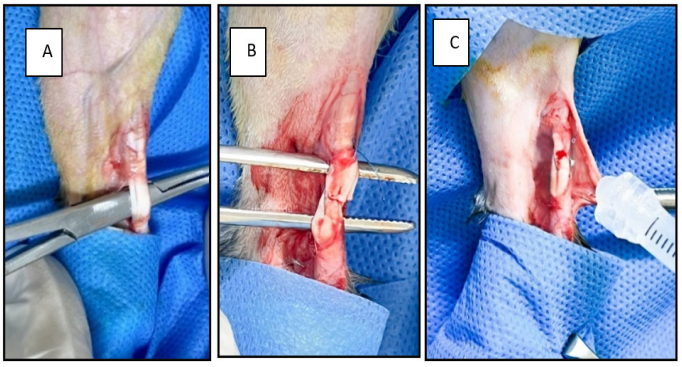

Figure 1: Intraoperative macroscopic images showing surgical exposure and treatment of the Achilles tendon. (A) A longitudinal skin incision is made over the Achilles region, and blunt dissection is performed to expose the tendon. (B) The tendon was repaired using the modified Kessler suture technique with USP 4.0 polypropylene suture. (C) Post-treatment phase with application of therapeutic nano encapsulated chitosan collagen hydrogel (0.3 ml) onto the exposed tendon prior to wound closure.

Postoperative care

Postoperative care included intramuscular administration of procaine penicillin at a dose of 40,000 IU/kg for three consecutive days (Carpenter *et al*., 2001). In addition, meloxicam was administered at a dose of 0.5 mg/kg (Liles *et al*., 2024). To support proper tendon healing, a cohesive bandage was applied with a gauze under to immobilize the operated limb at a 150-degree position and prevent

excessive movement (Trudel *et al*., 2007), every two days monitoring of the surgical site was conducted to check for signs of infection, wound dehiscence, or abnormal swelling (Thomopoulos *et al*., 2015). The rabbits were housed in individual cages and provided with standard veterinary post-surgical care, including appropriate nutrition and hydration.

Clinical assessment

Clinical assessment focused on passive mobilization and tendon gliding. Rabbits' operated limbs were immobilized at 150° flexion for three weeks, followed by controlled passive mobilization to evaluate tendon excursion, resistance, and smoothness of gliding during healing. This approach allows functional monitoring of adhesions and stiffness that impair tendon motion.

Clinical assessment was performed following immobilization, with tendon gliding of the operated limb. Each rabbit was observed for resistance during joint flexion and extension, and the smoothness of gliding was noted. This method provided a functional assessment of peritendinous adhesions and restoration of tendon excursion, which are considered the most direct clinical indicators of tendon healing. In animal models, such functional tests closely mimic the clinical evaluation of tendon repair in humans, as adhesions are a major cause of poor outcomes (Alhtheal *et al*., 2020). The ability to track mobility recovery non-invasively made this approach critical for correlating gross tendon function with subsequent structural findings (Tuncay *et al*., 2007).

Ultrasonography

Ultrasonographic images were captured using a F6 Vet unit with micro-convex probe with frequency range 5–7.5 MHz. Tendons were scanned in longitudinal planes from lateral approach. In longitudinal plane the ultrasound probe was placed slightly to the medial side to assure good visualisation of the Achilles tendon.

Ultrasound evaluation of normal and abnormal tendons was performed based on echogenicity (hyperechoic (bright) and hypoechoic (gray/dark)), tendon appearance, thickness, and collagen fiber organization. Normal tendons exhibited a uniformly bright, well-organized, and continuous fibrillar pattern. In contrast, abnormal tendons showed reduced or disrupted echogenicity, with darker areas, disorganized collagen structure, increased thickness, and irregular patterns with scattered hypoechoic regions. These ultrasonographic changes are characteristic of tendon pathologies such as tendinitis, tendinosis, tendon tears, adhesions, and post-surgical fibrosis.

Macroscopic assessment

At predetermined sacrifice timepoints that was taken at 1,4,8 and 12 weeks post operation, repaired tendons were carefully dissected for macroscopic evaluation of adhesion formation. Adhesions were graded according to the, ranging from Grade 0 (no adhesion) to Grade 4 (severe adhesions requiring sharp dissection). This system allowed direct quantification of adhesion severity and surgical dissection difficulty, thereby providing an objective measure of tendon gliding restoration. The Tang scoring system has been widely used in experimental tendon models and validated as a reliable metric to correlate with both histological and functional outcomes (Yang *et al*., 2016). This evaluation provided a clear picture of how each treatment influenced scar tissue formation and tendon mobility.

Histopathological assessment

Tendon specimens were processed for histopathological analysis using Hematoxylin and Eosin (H and E) and Masson's Trichrome (MT) staining. HandE staining enabled the evaluation of inflammatory response, vascular proliferation, and tenocyte morphology, while MT staining specifically highlighted collagen fiber deposition, orientation, and density. These histological markers are well-established indicators of tendon healing phases, beginning with inflammation, followed by fibroblast proliferation and ECM deposition, and culminating in collagen remodeling and maturation. By sampling at 1, 4, 8, and 12 weeks, it was possible to map the progression of healing across groups, and to distinguish between incomplete fibrotic repair and organized regenerative healing.

Statistical analysis

Statistical analysis was achieved by means of the Statistical Package for the Social Sciences (SPSS), version 25 (2019). The effect of treatment group and postoperative time period (and its interactions) on the parameters included in the adhesion scoring system were subjected to statistical analysis. The adhesion was scored using the scale described by Oryan and Moshiri (2012), and results are reported as means ± standard error (SE). Prior to analysis, data were examined for normality and homogeneity of variances using the Shapiro–Wilk test and Levene's test, respectively. A two-way analysis of variance (ANOVA) was applied to assess the main effects of treatment and time and their interaction on adhesion scores. When a statistically significant difference was detected, Least Significant Difference (LSD) post hoc test was used for multiple comparisons between group means. All statistical tests were two-tailed, and a probability value (P) of less than 0.05 was considered statistically significant. The results of the statistical analysis are presented in Table 1.

Table 1: Macroscopic adhesion grading system (Oryan and Moshiri, 2012).

Grade	Description
0	No adhesions
1	Mild adhesions
2	Moderate adhesions
3	Moderate to severe adhesions
4	Severe adhesions

RESULTS

Clinical evaluation

Clinical evaluation of the surgical sites in both groups revealed clear differences in inflammatory response and healing progression. However, no overt complications such as wound dehiscence, infection, or suture extrusion were observed in either group. Visual inspection of the incision lines confirmed clean wound margins and progressive wound closure throughout the healing period.

Following a 3-week immobilization period with the limb fixed at 150 degrees, assessments were performed to evaluate tendon gliding. In Group A (Control group), tendon gliding was markedly restricted. At week 4, animals displayed stiffness and resistance to passive flexion, suggesting adhesion formation and poor remodeling. By week 8, partial improvement was noted; however, gliding remained limited at week 12, although mobility slightly improved, residual restrictions persisted, reflecting incomplete resolution of adhesions.

In contrast, Group B (NECCH-treated) showed earlier and more substantial functional recovery. By week 4, smooth gliding with minimal resistance was observed, indicating reduced peritendinous adhesion and early matrix organization. At week 8, tendon excursion was nearly full, and by week 12, gliding was restored with no palpable resistance.

Importantly, the modified Kessler suturing technique, performed using USP 4.0 polypropylene suture, proved mechanically and biologically effective due to improved resistance to rupture under tension and advantageous of organized collagen deposition and minimal inflammation.

Macroscopic examination

Figures 2–5 illustrate the macroscopic examination at 1, 4, 8, and 12 weeks post-operation for both the control group (Group A) and the treated group (Group B, NECCH). Macroscopic examination of the control group at 1 week post-operation revealed severe adhesions between the tendon and surrounding tissues, with a mean adhesion score of 3.6 according to the grading system (Figure 6). These adhesions were dense, fibrous, and required sharp dissection, indicating extensive scar tissue formation and restricted tendon mobility (Figure 2A). In contrast, Group B (NECCH) at one week post operation showed moderate adhesions Graded 2.6 in the scoring system which were separable by blunt dissection (Figure 2B), while the results at four weeks post operation of Group A exhibit Grade 3.4 adhesions with persistent thickened, fibrotic tissue that requiring sharp dissection. However, Group B displayed notable improvement in which adhesions had decreased to 1.8 in the scoring system, were easily separable by blunt dissection (Figure 3A, B).

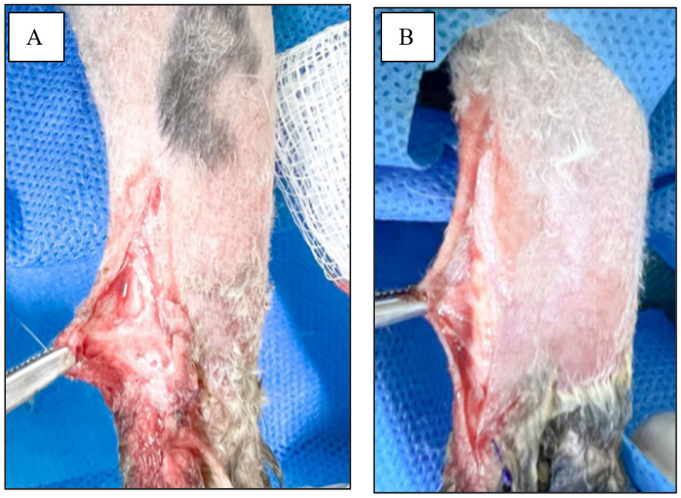

Figure 2: (A) Macroscopic evaluation of tendon adhesion at 1 week post-operation in the control group shows severe adhesion Graded 3.6 requiring sharp dissection. (B) Macroscopic evaluation of tendon adhesion at 1 week post-operation in the NECCH group shows moderate adhesion Grade 2.6 requiring sharp dissection.

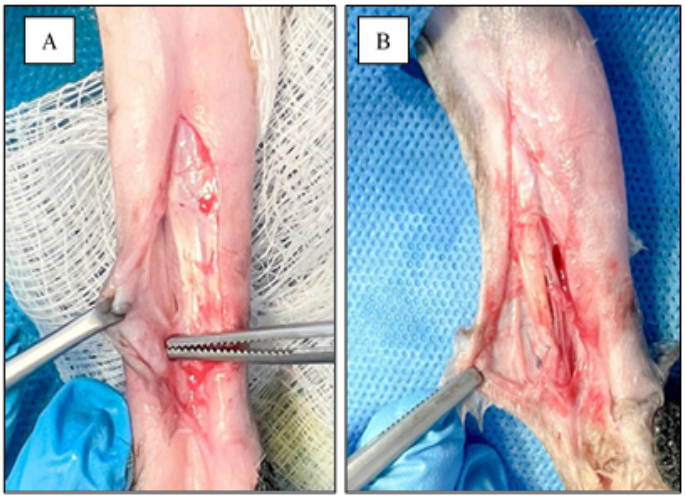

Figure 3: (A) Macroscopic evaluation of tendon adhesion at 4 weeks post-operation in the control group shows moderate to severe adhesion Graded 3.4 requiring sharp dissection. (B) Macroscopic evaluation of tendon adhesion at 4 weeks post-operation in the NECCH group shows moderate adhesion Graded 1.8 requiring blunt dissection.

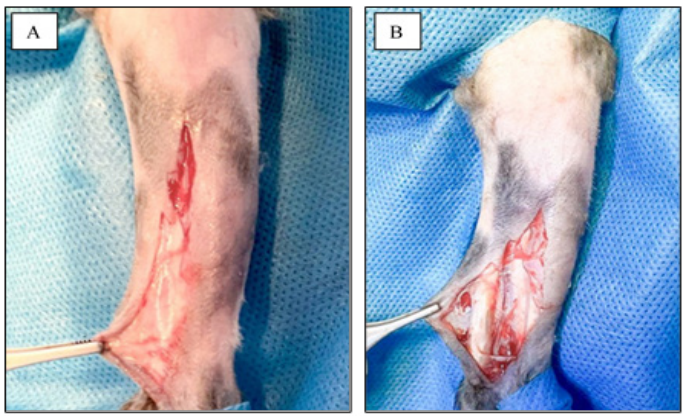

Figure 4: (A) Macroscopic evaluation of tendon adhesion at 8 weeks post-operation in the control group shows persistent adhesion Graded 3.2 requiring sharp dissection. (B) Macroscopic evaluation of tendon adhesion at 8 weeks post-operation in the NECCH group shows reduced adhesion Graded 1.4 requiring manual dissection.

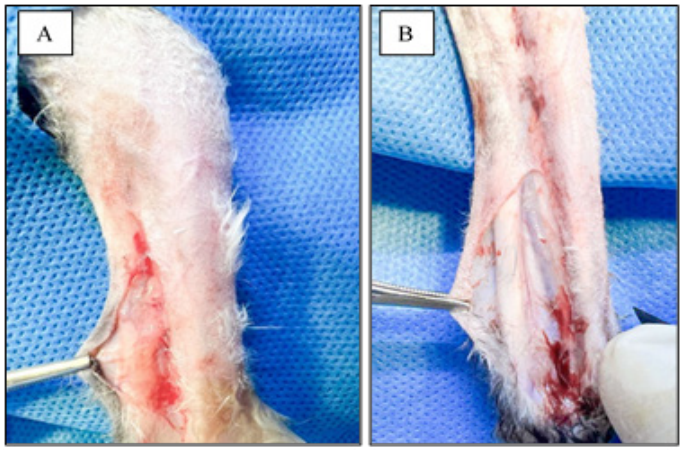

Figure 5: (A) Macroscopic evaluation of tendon adhesion at 12 weeks post-operation in the control group shows permanent adhesion Graded 3.2 requiring sharp dissection. (B) Macroscopic evaluation of tendon adhesion at 12 weeks post-operation in the NECCH group shows minimal to near absence adhesion Graded 0.60 with restored morphology.

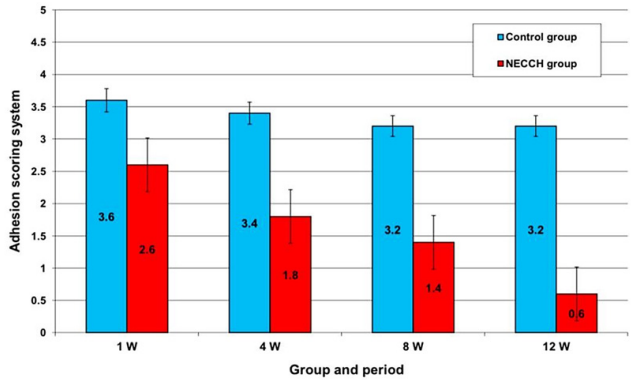

Figure 6: Adhesion scoring system grades demonstrated that Group B (NECCH-treated) consistently showed lower adhesion scores and superior healing compared to Group A throughout all evaluation periods.

At 8 weeks post-operation, adhesions in Group A were graded at 3.2, characterized by dense fibrotic tissue. In contrast, Group B exhibited significantly fewer adhesions, with a mean grade of 1.4 and minimal fibrosis (Figure 4A, B). At 12 weeks, adhesions in Group A persisted and remained graded at 3.2, with separation requiring blunt dissection. Meanwhile, Group B demonstrated near-complete tendon healing, with a markedly reduced adhesion score of 0.6 and a smooth tendon surface. In this group, dissection was easily performed manually (Figure 5A, B).

Ultrasound evaluation

Ultrasound evaluation result at 1 week post operation of Group A (Figure 7A) showed hypoechoic regions with irregular tendon margins, reflecting edema, necrosis, and disrupted collagen structure. In contrast, Group B (Figure 7B) displayed progressive and organized improvements. At week 1, mild hyperechogenicity was noted, likely associated with the collagen component of NECCH. Moreover, ultrasound results at 4 weeks post operation in Group A (Figure 8A) remained hypoechoic areas with irregular margins and several fibrotic bands, indicating ongoing scarring and adhesions. Meanwhile, Group B (Figure 8B) showed more organized echotexture, less hypoechoic areas and near-normal tendon borders. While the ultrasound results At 8 weeks post operation in Group A (Figure 9A) continued to exhibit poorly defined tendon boundaries, disrupted tendon surface, and irregular echogenicity. In contrast, Group B (Figure 9B) tendons demonstrated well-aligned hyperechoic fibers, minimal fibrotic signs, and clear regular tendon surface. By week 12 post operation, Group A tendons (Figure 10A) still displayed irregular tendon surface, while Group B (Figure 10B) showed near-normal echotexture, uniform, regular tendon surface alignment, and an absence of adhesions.

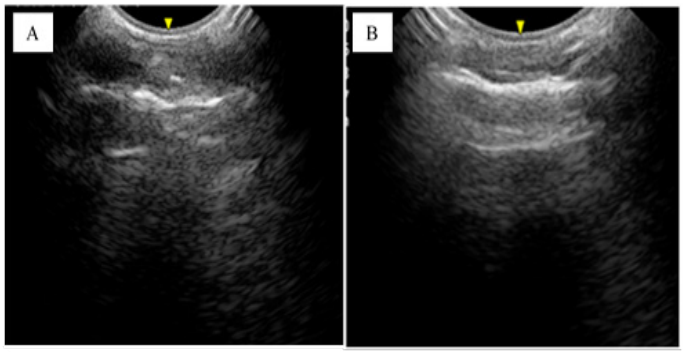

Figure 7: (A) The ultrasound image 1 week postoperation shows Hypoechoic tendon region with irregular margins and disrupted tendon architecture and poor initial healing. (B) The ultrasound image 1 week postoperation shows Hypoechoic tendon with slightly irregular margins than Group A. Despite surgical disruption

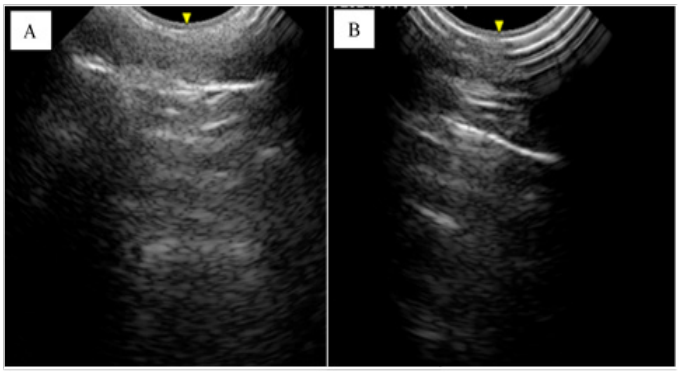

Figure 8: (A) The ultrasound image 4 weeks postoperation shows Hypoechoic region with poorly defined tendon margins and disrupted pattern. (B) The ultrasound image 4 weeks postoperation shows echogenic tendon with clear structure beginning to reform. smooth contours suggest early remodeling

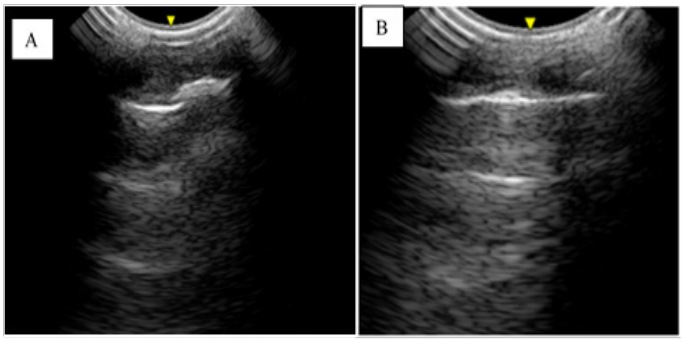

Figure 9: (A) The ultrasound image 8 weeks postoperation shows irregular tendon surface and disrupted pattern, reflecting slow tissue regeneration. (B) The ultrasound image 8 weeks postoperation shows Well-aligned tendon surface and normalized echogenicity, indicating advanced healing.

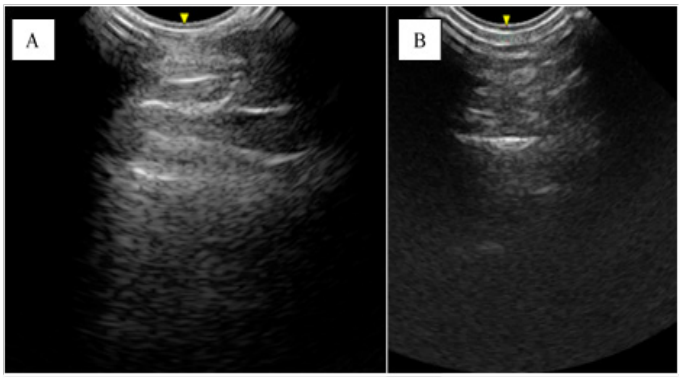

Figure 10: (A) The ultrasound image 12 weeks postoperation shows Tendon margins partially restored, but texture remains inconsistent with areas of hypoechogenicity, suggesting incomplete remodeling. (B) The ultrasound image 12 weeks postoperation shows Tendon architecture nearly identical to healthy tissue, with uniform echogenicity and clear surface continuity, evidence of near complete recovery.

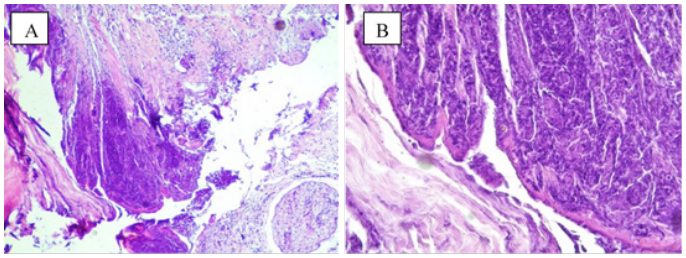

Figure 11: Control Group (group A) 1 week post operation. (A) The histopathological section shows obvious changes of collagen fibers., increased tenocyte numbers, presence of inflammatory cells and plasma cells. (H and E stain 10X). (B) The histopathological section shows Numerous rounded tenocytes with dark nuclei are scattered, indicating poor cellular alignment and ongoing inflammation. (H and E stain 40X).

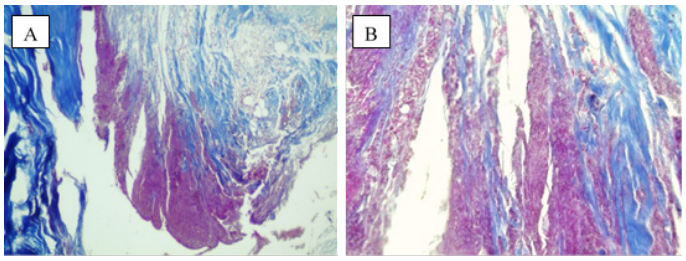

Figure 12: Control Group (group A) 1 week post operation. (A) the histopathological section shows Collagen deposition irregular. Blue-stained collagen fibers lack directional orientation, and there is clear evidence of tissue disorganization (MT stain 10X). (B) collagen fibers are poorly compacted with wide interfibrillar spaces with presence of loosely packed fibroblasts (MT stain 40X).

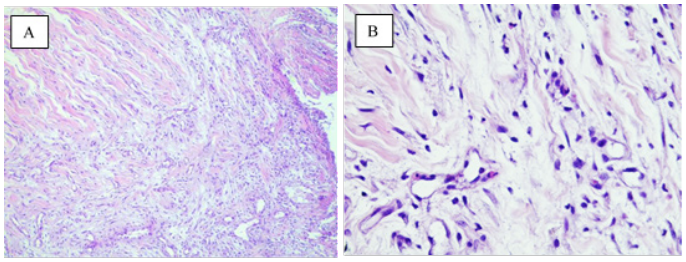

Figure 13: NECCH Group (Group B) 1 week post operation. (A) The histopathlogical section shows presence of collagen alignment in non paralled arrangment which is clearly visible, also lack of fibroplast, and revasculorization. (HandE stain 10X,). (B) The histopathlogical section shows the tenocyte nuclear morphology is typical of the early proliferative phase of tendon healing (H and E stain 40X).

Histopathological evaluation

Histopathological examination of tendon tissue was performed at 1, 4, 8, and 12-weeks post-operation for both the control (Group A) and treated (Group B, NECCH) groups using Hematoxylin and Eosin (H and E) and Masson's Trichrome (MT) staining to evaluate cellular

response, vascularization, and collagen organization (illustrations were presented in the form of Figures 11-26). Tendon healing was assessed histologically at 1, 4, 8, and 12-weeks post-operation in both groups. H and E stained sections from Group A (control) showed marked temporal changes in tendon healing. At 1-week post-operation, sections revealed disorganized and fragmented collagen fibers with wide interfibrillar spaces and a predominance of rounded, hyperchromatic tenocyte nuclei, indicating acute inflammation and early granulation tissue formation (Figure 11A, B). By week 4, partial maturation of fibrous tissue was observed; however, collagen bundles remained loosely arranged, and tenocytes displayed variable morphology, suggesting incomplete remodeling (Figure 15A, B). At 8 weeks, collagen fibers exhibited partial alignment, although irregular distribution and residual rounded tenocyte morphology persisted, reflecting delayed matrix organization (Figure 19A, B). By 12 weeks, some fiber compaction and the appearance of spindle-shaped nuclei were evident; nevertheless, the tissue continued to show inconsistent collagen alignment and signs of incomplete structural restoration (Figure 23A, B).

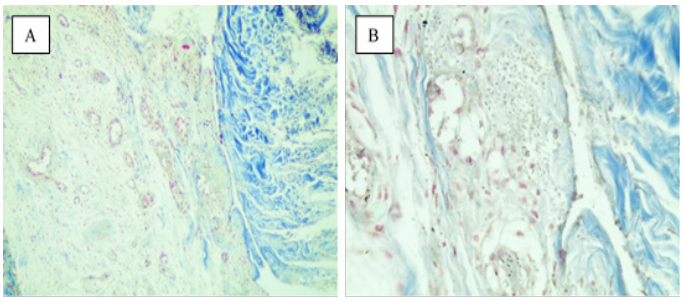

Figure 14: NECCH Group (Group B) 1 week post operation (A) The histopathlogical section shows Collagen fibers and new capilleries formation. (B) the histopathological section shows faint, patchy blue staining with loosely arranged collagen fibers and minimal matrix density.

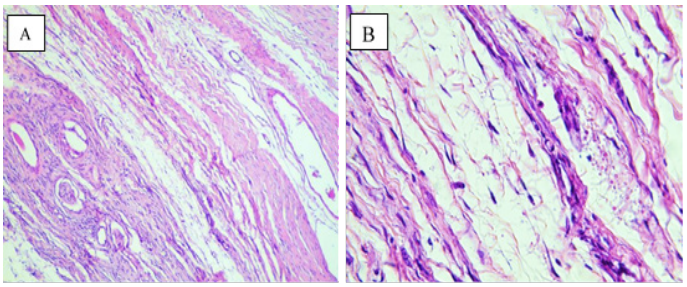

Figure 15: Control Group (group A) 4 weeks post operation. (A) The histopathlogical section shows the tendon loosely arranged and disorganized collagen fibers, with uneven orientation and persistent interfibrillar gaps (H and E 10X). (B) The histopathlogical section shows tenocyte with their rounded nuclei suggesting incomplete transition into the remodeling phase with reduced inflamation. (H and E stain 40X).

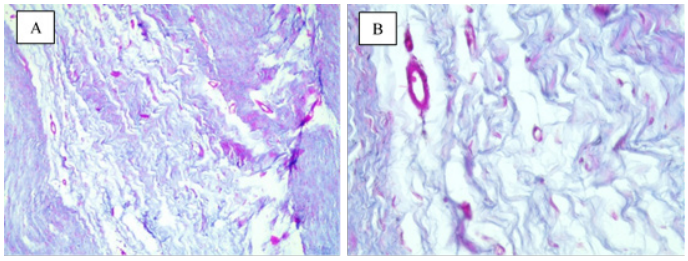

Figure 16: Control Group (group A) 4 weeks post operation. (A) The histopathlogical section shows Irregular and fragmented collagen fibers with faint blue staining, reflecting slow and incomplete remodeling (MT stain 10X). (B) collagen bundles appear fragmented with widened interfibrillar spaces, and no evidence of clear alignment is observed (MT stain 40X).

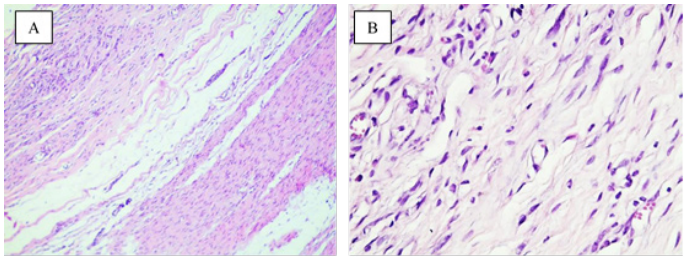

Figure 17: NECCH Group (group B) 4 weeks post operation. (A) The histopathlogical section shows well-aligned collagen fibers with a more compact extracellular matrix compared to the control group (H and E stain 10X). (B) The histopathlogical section shows tenocytes with predomination typical elongated nuclei and new formation of capilleries. (H and E stain 40X).

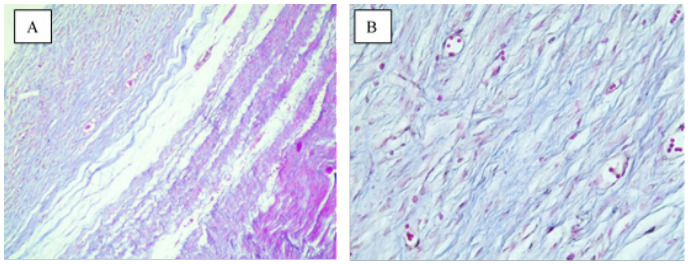

Figure 18: NECCH Group (group B) 4 weeks post operation. (A) The histopathlogical section shows collagen fibers appear densely packed and more uniformly stained in blue, indicating enhanced matrix deposition and alignment (MT stain 10X). (B) The histopathlogical section shows collagen bundles exhibit organization and continuity, with minimal interfibrillar gaps with Elongated tenocyte nuclei are visible between the fibers (MT stain 40X).

The MT-stained sections in Group A (Control), at week 1 showed faint, patchy blue staining with loosely arranged collagen fibers and minimal matrix density, indicating delayed extracellular matrix (ECM) synthesis (Figure 12-A, B). At week 4, moderate collagen deposition was noted, yet fiber alignment remained irregular, and the staining pattern was uneven (Figure 16A, B). By weeks 8 and 12,

although the intensity of collagen staining improved, the overall fiber architecture remained disrupted, with areas of loosely packed and discontinuous bundles (Figures 20 and 24A, B).

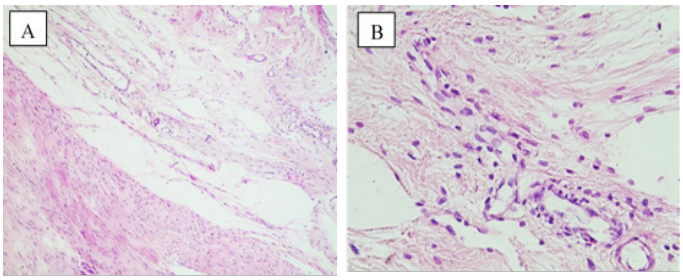

Figure 19: control Group (group A) 8 weeks post operation. (A) The histopathlogical section shows Disorganized collagen fibers, Loosely packed collagen, capillary proliferation, persistent vascularization and incomplete remodeling. (H and E stain 10X). (B) the histopathological section shows tenocyte nuclei appear a little elongated but still vary in shape and orientation, indicating incomplete remodeling (HandE stain 40X).

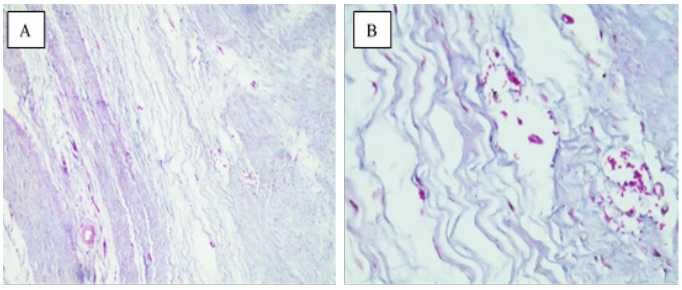

Figure 20: control Group (group A) 8 weeks post operation. (A) the histopathological section shows collagen fibers unevenly stained and loosely arranged with limited alignment, suggesting delayed matrix maturation (MT stain 10X). (B) the histopathological section shows blue-stained collagen bundles partially fragmented and interspersed with disorganized tenocyte nuclei (MT stain 40X).

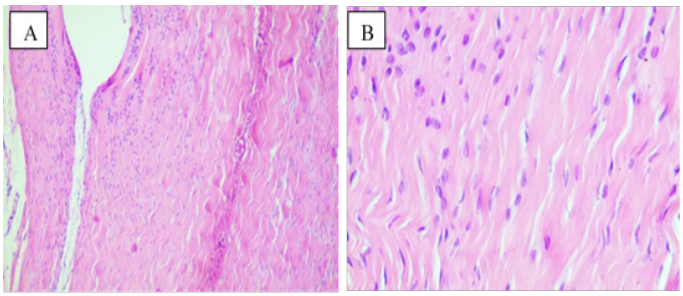

Figure 21: NECCH Group (group B) 8 weeks post operation. (A) The histopathlogical section shows Oriented collagen bundles and reduced inflammation, indicating tissue maturation (H and E stain 10X). (B) the histopathological section shows tenocyte nuclei uniformly elongated and spindle-shaped, aligned parallel to the collagen bundles (H and E stain 40X).

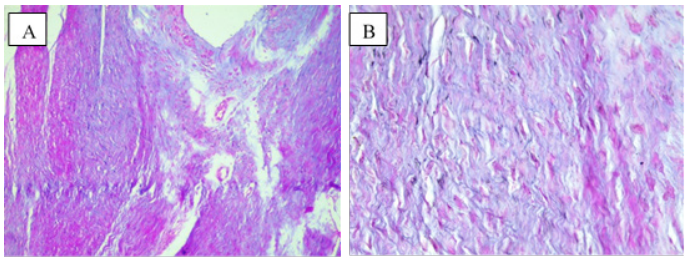

Figure 22: NECCH Group (group B) 8 weeks post operation (A) The histopathlogical section shows Aligned, well-structured collagen bundles stained deep blue, consistent (MT stain 10X). the histopathological section shows collagen bundles compact and parallel, with elongated, spindle-shaped tenocyte nuclei embedded between them (MT stain 40X).

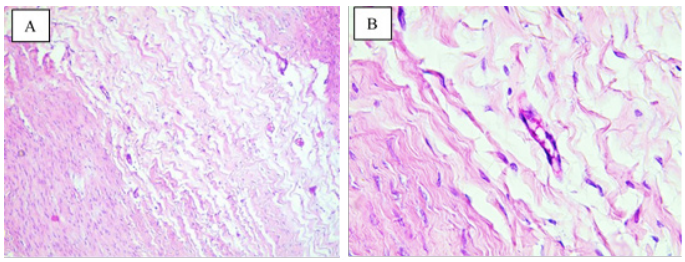

Figure 23: Control Group (group A) 12 weeks post operation. (A) The histopathalogical section shows partially organized collagen fibers with waviness and interfibrillar spacing (H and E stain 10X). (B) The histopathalogical section shows tenocyte nuclei appear variably shaped some elongated, others rounded indicating ongoing, though incomplete, remodeling (H and E stain 10X).

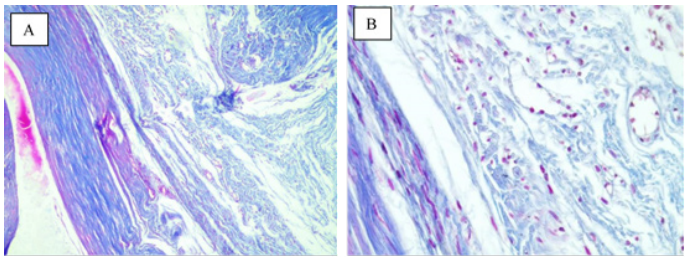

Figure 24: Control Group (group A) 12 weeks post operation. (A) The histopathalogical section shows collagen fibers aligned but remain loosely arranged, with faint blue staining indicating incomplete matrix densification. The overall structure lacks compact fiber bundling (MT stain 10X). (B) The histopathalogical section shows collagen bundles are discontinuous and interspersed with irregularly shaped tenocyte nuclei, some remain rounded (MT stain 40X).

In contrast, H and E stain sections, in Group B (NECCH-treated) demonstrated more favorable histological features at each time point. At 1 week, the tendon sections already displayed fiber density and initial parallel fiber orientation, with tenocyte nuclear morphology is typical of the early proliferative phase of tendon healing (Figure

13A, B). By 4 weeks, collagen bundles appeared well-aligned and densely packed, with consistently elongated tenocyte nuclei embedded in an organized extracellular matrix (Figure 17A, B). At 8 and 12 weeks, the tissue architecture in Group B closely resembled native tendon structure, marked by compact, parallel collagen alignment and uniformly distributed spindle-shaped tenocytes (Figures 21 and 25A, B). The MT stain sections of Group B (NECCH-treated) demonstrated enhanced collagen maturation at all timepoints. As early as week 1, more intense and continuous blue staining was visible, reflecting accelerated ECM deposition (Figure 14A, B). By week 4, the collagen fibers were densely packed and better aligned, forming organized bundles (Figure 18A, B). At weeks 8 and 12, MT-stained sections from Group B revealed highly organized, compact collagen fibers with uniform staining intensity, closely mimicking native tendon structure (Figures 22 and 26A, B). The consistent and dense collagen staining across the healing period confirms the regenerative effect of NECCH on tendon matrix quality, promoting advanced remodeling and tissue strength.

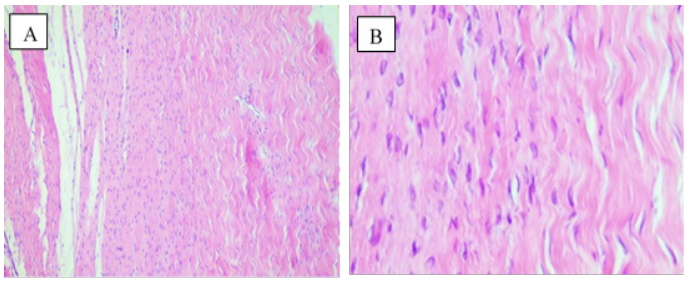

Figure 25: NECCH Group (group B) 12 weeks post operation. (A) The histopathlogical section shows dense, parallel collagen fiber alignment with minimal interfibrillar spaces (H and E stain 10X). (B)The histopathlogical section shows elongated spindle-shaped tenocyte nuclei are aligned within the fibers, indicating advanced remodeling and cellular organization (H and E stain 40X)

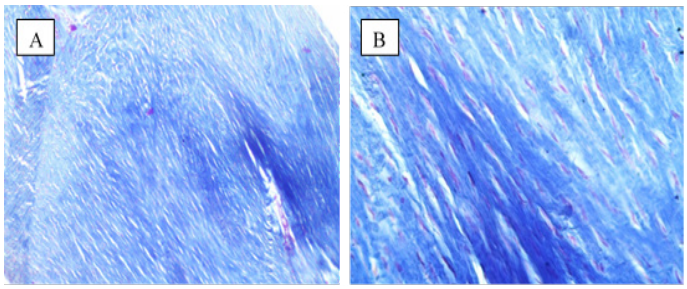

Figure 26: NECCH Group (group B) 12 weeks post operation. (A) The histopathlogical section shows collagen bundles deeply stained in blue and appear compact and directionally aligned at both magnifications (MT stain 10X). (B) The histopathlogical section shows tenocytes clearly embedded between the bundles with minimal distortion (MT stain 40X).

DISCUSSION

Postoperative management plays a critical role in determining the functional outcome of tendon repair. In this study, a cohesive bandage was applied to maintain the hind limb at 150° of flexion, ensuring controlled mechanical tension across the Achilles tendon repair site. After a three-week immobilization period, gradual passive limb mobilization was initiated to promote tendon gliding and stimulate physiological remodeling. Some literature advocates for extended immobilization to minimize the risk of rerupture (Andarawis-Puri *et al*., 2015). However, the results of this study support a more contemporary perspective that early, gentle mobilization can enhance healing without compromising repair strength. Improved tendon excursion in Group B, as compared to the restricted gliding observed in Group A, reinforces the benefits of early mobilization when combined with bioactive treatment. Group B, which received Nano-Encapsulated Chitosan-Collagen Hydrogel (NECCH), demonstrated smoother, freer tendon movement. This improvement aligns with the known anti-adhesive and anti-inflammatory effects of chitosan, along with the structural support provided by collagen. Together, these components contributed to a more organized extracellular matrix and reduced fibrotic interference. These outcomes are in agreement with the findings of Deepthi *et al*. (2016) and Xia *et al*. (2022), who reported enhanced tendon gliding and reduced adhesion formation following hydrogel-based treatments in vivo. Additionally, the use of the modified Kessler suture technique with USP 4.0 polypropylene provided robust mechanical coaptation with minimal inflammatory response. This finding concurs with Millar *et al*. (2021), who reported that this suture pattern offers superior tensile strength and biocompatibility in tendon repair.

Tendon adhesions are primarily caused by excessive inflammation and extrinsic fibroblast infiltration during the early phases of healing, leading to disorganized extracellular matrix deposition and fibrotic tissue formation between the tendon and surrounding structures (Stoll *et al*., 2011; Andarawis-Puri *et al*., 2015). These adhesions typically begin forming within the first few weeks post-injury and mature into restrictive fibrotic bands by weeks 8–12. The application of NECCH has been shown to mitigate these effects by modulating the inflammatory response and supporting organized collagen remodeling. Chitosan reduces pro-inflammatory cytokine expression, while collagen provides a scaffold that promotes tenocyte proliferation and matrix alignment (Ricard-Blum, 2011; Xia *et al*., 2022). Studies have demonstrated that NECCH-treated tendons exhibit less thickening, fewer adhesions, and improved tendon gliding, suggesting a shift toward intrinsic healing and functional tissue regeneration (Deepthi *et al*., 2016; Freedman *et al*., 2022). While some

protocols still recommend prolonged immobilization to prevent re-rupture, our findings support early motion in combination with bioactive like NECCH, which appears to reduce fibrosis without compromising mechanical integrity.

The persistent, dense adhesions observed in Group A throughout all time points reflect a chronic fibrotic response and lack of effective remodeling. Such adhesions are linked to unregulated fibroblast proliferation and excessive extracellular matrix (ECM) deposition, which compromise tendon mobility and healing outcomes (Galatz *et al*., 2015; Alkhilani and Atta, 2020). The Grade 4 adhesions and tendon thickening support findings from earlier studies on fibrotic tendon repair under inflammatory conditions (Andarawis-Puri *et al*., 2015).

In contrast, Group B (NECCH-treated) showed significantly improved outcomes, particularly by weeks 4 through 12. These improvements can be attributed to the anti-inflammatory and anti-fibrotic properties of chitosan and the tissue-regenerating potential of collagen. Chitosan has been previously shown to modulate immune responses and reduce scar formation during tendon healing (Xia *et al*., 2022), while collagen-based hydrogels provide a structural scaffold that promotes fibroblast proliferation and organized ECM deposition (Lee *et al*., 2001; Ricard-Blum, 2011).

The reduction in adhesion severity and restoration of tendon morphology in Group B align with research indicating the role of bioactive hydrogels in enhancing ECM remodeling, minimizing fibrosis, and supporting tendon gliding (Hu *et al*., 2023). The nearly complete tendon regeneration and low adhesion scores observed by week 12 in Group B confirm the efficacy of NECCH in promoting functional and structural recovery.

The ultrasound findings highlight the limited healing capacity in untreated tendons, as observed in Group A, where persistent hypoechoic changes and disorganized collagen fibers indicate prolonged inflammation and chronic fibrosis. These findings align with previous literature describing the detrimental impact of unregulated inflammation and poor extracellular matrix (ECM) remodeling in tendon injuries (Andarawis-Puri *et al*., 2015). In contrast, Group B benefited from the anti-inflammatory and tissue-structuring properties of nano-encapsulated chitosan-collagen hydrogel (NECCH). The preservation of fibrillar structure and reduced swelling in early stages suggest that NECCH modulates early inflammatory responses and supports collagen alignment, which is critical for successful healing (Xia *et al*., 2022). The improved collagen organization and tendon margin clarity observed at 4 and 8 weeks indicate active ECM remodeling and reduced adhesion formation, consistent with findings on collagen-based biomaterials (Lee *et al*., 2001; Ricard-Blum, 2011). By week 12, the complete restoration of tendon structure in Group B underscores NECCH's long-term effectiveness in preventing peritendinous adhesions and promoting functional tissue regeneration (Schneider *et al*., 2018; Freedman *et al*., 2022). These results demonstrate that NECCH not only enhances the healing timeline but also improves final tendon quality.

The histopathological analysis across all timepoints revealed substantial differences in tendon healing progression between the control (Group A) and NECCH-treated group (Group B). In Group A, early sections demonstrated typical features of acute tendon injury, including disorganized collagen deposition, rounded tenocyte nuclei, and widespread inflammatory infiltration. These findings persisted into later stages, with 8- and 12-week sections still showing partial collagen alignment, irregular nuclear morphology, and evident interfibrillar gaps, indicating prolonged inflammation and incomplete remodeling.

In contrast, Group B exhibited a more favorable histological profile at every phase of healing. By week 1, early signs of collagen alignment and fibroblast elongation were already visible, suggesting a more rapid transition from inflammation to proliferation. At 4 and 8 weeks, collagen fibers in Group B were notably more organized and densely packed, with spindle-shaped tenocyte nuclei aligned along the fiber axis hallmarks of active matrix remodeling. By week 12, histological architecture closely resembled that of normal tendon, reflecting successful tissue regeneration promoted by the NECCH application.

These findings are consistent with prior studies demonstrating the regenerative potential of chitosan-based hydrogels in modulating the inflammatory response, supporting cellular alignment, and enhancing extracellular matrix (ECM) maturation. For instance, Deepthi *et al*. (2016) showed that a chitosan–collagen composite hydrogel improved fiber orientation and tenocyte morphology in a rat tendon model. Similarly, Xia *et al*. (2022) reported that chitosan's anti-inflammatory and bioadhesive properties promote favorable cellular environments for tendon healing.

However, some studies suggest that while collagen-based scaffolds may support early regeneration, their long-term mechanical integration remains uncertain without crosslinking or reinforcement. Kaux *et al*. (2011) noted that hydrogels lacking structural reinforcement may degrade prematurely, potentially compromising long-term remodeling. Despite this, our results suggest that

NECCH, with the suitable suture material and modified Kessler technique even without any other additional synthetic crosslinkers, provided sufficient matrix stability over the 12-week healing period.

CONCLUSION

In conclusion, the histological evaluation supports the effectiveness of NECCH in enhancing tendon healing through improved collagen organization and tenocyte alignment. This suggests that bioactive nano-encapsulated hydrogels may serve as a promising single-application adjunct for tendon regeneration. Future work should investigate the mechanical properties of the repaired tendon to correlate histological improvements with functional outcomes.

ACKNOWLEDGEMENT

The authors express their gratitude to the staff of the University of Baghdad's College of Veterinary Medicine for their assistance in this task.

NOVELTY STATEMENT

This study presents a novel nano-encapsulated chitosan-collagen hydrogel (NECCH) as a single-application, injectable scaffold for improving Achilles tendon repair in a rabbit model. Unlike previous studies that utilized separate biomaterial components or required multiple applications, this research combines chitosan and collagen into a bioactive nanocomposite using ionic gelation with tripolyphosphate (TPP), enabling sustained local delivery and structural integration at the repair site. The study uniquely validates the in vivo biostability, bioavailability, and regenerative efficacy of NECCH through detailed physicochemical (SEM, FTIR, UV-Vis, HPLC) and biological (clinical, ultrasound, macroscopic, histopathological) analyses. The findings construct NECCH as a biocompatible, anti-inflammatory, and anti-adhesive scaffold that significantly develops collagen organization, reduces adhesion formation, and restores tendon architecture offering a minimally invasive alternative to traditional grafts or systemic therapies for tendon healing. This work is among the firs. provide comprehensive mechanistic and morphological validation of nano-encapsulated chitosan-collagen hydrogel in tendon regeneration.

AUTHOR'S CONTRIBUTION

The authors contributed equally.

Generative AI and AI-assisted technology statement

The authors declare that no generative AI or AI-assisted technologies were used in the preparation, writing, analysis, or interpretation of this manuscript.

Conflict of interest

The authors have declared no conflict of interest.

REFERENCES

Al-Falahi NH (2016). A comparative biomechanical study of repaired tendons wrapped with two biological matrices in bucks. Iraqi J. Vet. Med., 40(1): 73–78. https://doi.org/10.30539/iraqijvm.v40i1.141

Alhtheal ED, Azhar JB (2018). Effect of zinc oxide nanoparticles prepared from zinc sulphate against gram-positive and gram-negative microorganisms *in vitro*. Iraqi J. Vet. Med., 42(1): 18–22. https://doi.org/10.30539/iraqijvm.v42i1.25

Alhtheal ED, Radhy AM, Hasan MS, Kareem MH, Saleh EN (2020). Therapeutic effects of olive oil on rabbit with lead toxicity. Int. J. Pharma. Res., 12(1). https://doi.org/10.31838/ijpr/2020.12.01.188

Alkhilani MA, Atta NM (2020). Evaluation of the effect of low power laser irradiation on healing of induced tendon injuries in rabbits. Iraqi J. Vet. Med., 44(E0): 113–122. https://doi.org/10.30539/ijvm.v44i(E0).1459

Andarawis Puri N, Nelly ELF, Louis JS (2015). Tendon basic science: Development, repair, regeneration, and healing. J. Orthop. Res., 33(6): 780–784. https://doi.org/10.1002/jor.22869

Carpenter JW, Mashima TY, Rupiper DJ (2001). Exotic animal formulary. 2nd ed. W.B. Saunders.

Deepthi S, Sundaram MN, Kadavan JD, Jayakumar R (2016). Layered chitosan-collagen hydrogel/aligned PLLA nanofiber construct for flexor tendon regeneration. Carbohydr. Polym., 153: 492–500. https://doi.org/10.1016/j.carbpol.2016.07.124

Egwu CO, Aloke C, Onwe KT, Umoke CI, Nwafor J, Eyo RA, Okoro CO (2024). Nanomaterials in drug delivery: Strengths and opportunities in medicine. Molecules, 29(11): 2584. https://doi.org/10.3390/molecules29112584

Freedman BR, Kuttler A, Beckmann N, Nam S, Kent D, Schuleit M, Mooney DJ (2022). Enhanced tendon healing by a tough hydrogel with an adhesive side and high drug-loading capacity. Nat. Biomed. Eng., 6(10): 1167–1179. https://doi.org/10.1038/s41551-021-00810-0

Galatz LM, Gerstenfeld L, Heber-Katz E, Rodeo SA (2015). Tendon regeneration and scar formation: The concept of scarless healing. J. Orthop. Res., 33(6): 823–831. https://doi.org/10.1002/jor.22853

Hassan MA, Abd Elkawi M, Saber MS, Senosy W, Nassif M, El-Sherif MW (2024). Evaluation of xylazine-ketamine anesthesia in rabbits undergoing tendon surgery. New Valley Vet. J., 4(1): 7. https://doi.org/10.21608/nvvj.2023.247402.1038

Hu J, Liu S, Fan C (2023). Applications of functionally-adapted hydrogels in tendon repair. Front. Bioeng. Biotechnol., 11: 1135090. https://doi.org/10.3389/fbioe.2023.1135090

Kaux, J. F., Forthomme, B., Le Goff, C., Crielaard, J. M., Croisier, J. L. (2011). Current opinions on tendinopathy. Journal of

sports science & medicine, 10(2), 238.
Lee CH, Singla A, Lee Y (2001). Biomedical applications of collagen. Int. J. Pharm., 221(1–2): 1–22. https://doi.org/10.1016/S0378-5173(01)00691-3
Liles M, Brown S, Di Girolamo N (2024). Administration of meloxicam before rather than after castration on eating, defecation and pain indicators in pet rabbits. Vet. Med. Sci., 10(2): e1354. https://doi.org/10.1002/vms3.1354
Millar NL, Murrell GAC, McInnes IB (2017). Inflammatory mechanisms in tendinopathy towards translation. Nat. Rev. Rheumatol., 13(2): 110–122. https://doi.org/10.1038/nrrheum.2016.213
Millar, N. L., Silbernagel, K. G., Thorborg, K., Kirwan, P. D., Galatz, L. M., Abrams, G. D., Rodeo, S. A. (2021). Tendinopathy. Nature reviews Disease primers, 7(1), 1. https://doi.org/10.1038/s41572-020-00234-1
Oryan, A., Moshiri, A., Parizi, A. H. M., Jahromi, A. R. (2012). Repeated administration of exogenous Sodium-hyaluronate improved tendon healing in an in vivo transection model. Journal of Tissue Viability, 21(3), 88-102. https://doi.org/10.1016/j.jtv.%202012.06.002"https://doi.org/10.1016/j.jtv. 2012.06.002
Parchi PD, Vittorio O, Andreani L, Battistini P, Piolanti N, Marchetti S, Lisanti M (2016). Nanoparticles for tendon healing and regeneration: Literature review. Front. Aging Neurosci., 8: 202. https://doi.org/10.3389/fnagi.2016.00202
Ricard-Blum S (2011). The collagen family. Cold Spring Harb. Perspect. Biol., 3(1): a004978. https://doi.org/10.1101/cshperspect.a004978
Salih SI, E'atelaf A, Mahdi AK, Ra S (2015). Role of chitosan application in postoperative abdominal adhesions in rabbits. Iraqi. J. Vet. Med., 39(1): 105–111. https://doi.org/10.30539/iraqijvm.v39i1.206
Sánchez-Cid P, Jiménez-Rosado M, Rubio-Valle JF, Romero A, Ostos FJ, Rafii-El-Idrissi Benhnia M, Perez-Puyana V (2022). Biocompatible and thermoresistant hydrogels based on collagen and chitosan. Polymers, 14(2): 272. https://doi.org/10.3390/polym14020272
Schneider, M., Angele, P., Järvinen, T. A., Docheva, D. (2018). Rescue plan for Achilles: Therapeutics steering the fate and functions of stem cells in tendon wound healing. Advanced drug delivery reviews, 129, 352-375.
Stoll C, John T, Conrad C, Lohan A, Hondke S, Ertel W, Schulze-Tanzil G (2011). Healing parameters in a rabbit partial tendon defect following tenocyte/biomaterial implantation. Biomaterials, 32(21): 4806–4815. https://doi.org/10.1016/j.biomaterials.2011.03.026
Thomopoulos, S., Parks, W. C., Rifkin, D. B., & Derwin, K. A. (2015). Mechanisms of tendon injury and repair. Journal of Orthopaedic Research, 33(6), 832-839. https://doi.org/10.1002/jor.22806
Trudel G, Koike Y, Ramachandran N, Doherty G, Dinh L, Lecompte M, Uhthoff HK (2007). Mechanical alterations of rabbit Achilles' tendon after immobilization correlate with bone mineral density but not with imaging. Arch. Phys. Med. Rehabil., 88(12): 1720–1726. https://doi.org/10.1016/j.apmr.2007.07.034
Tuncay, I., Kucuker, H., Uzun, I., Karalezli, N. (2007). The fascial band from semitendinosus to gastrocnemius: the critical point of hamstring harvesting an anatomical study of 23.
Xia Y, Wang D, Liu D, Su J, Jin Y, Wang D, Liu B (2022). Applications of chitosan and its derivatives in skin and soft tissue diseases. Front. Bioeng. Biotechnol., 10: 894667. https://doi.org/10.3389/fbioe.2022.894667
Yang G, Rothrauff BB, Lin H, Yu S, Tuan RS (2017). Tendon-derived extracellular matrix enhances TGF-β3-induced tenogenic differentiation of human adipose-derived stem cells. Tissue Eng. Part A, 23(3–4): 166–176. https://doi.org/10.1089/ten.tea.2015.0498
Yang G, Rothrauff BB, Lin H, Yu S, Tuan RS (2017). Tendonderived extracellular matrix enhances TGF-β3-induced tenogenic differentiation of human adipose-derived stem cells. Tissue Eng. Part A, 23(3–4): 166–176. https://doi.org/10.1089/ten.tea.2015.0498
Zhang, M., An, H., Zhang, F., Jiang, H., Wan, T., Wen, Y., Zhang, P. (2023). Prospects of using chitosan-based biopolymers in the treatment of peripheral nerve injuries. International Journal of Molecular Sciences, 24(16), 12956. https://doi.org/10.3390/ijms241612956